

HUPD-0012

# $B \rightarrow \pi\rho, \pi\omega$ Decays in Perturbative QCD Approach

Cai-Dian Lü, Mao-Zhi Yang

Theory Division, Institute of High Energy Physics, Chinese Academy of Sciences,  
P.O. Box 918(4), Beijing 100039, China \*

and

Physics Department, Hiroshima University, Higashi-Hiroshima 739-8526, Japan

December 2, 2024

## Abstract

We calculate the branching ratios and CP asymmetries for  $B^0 \rightarrow \pi^+\rho^-$ ,  $B^0 \rightarrow \rho^+\pi^-$ ,  $B^+ \rightarrow \rho^+\pi^0$ ,  $B^+ \rightarrow \pi^+\rho^0$ ,  $B^0 \rightarrow \pi^0\rho^0$ ,  $B^+ \rightarrow \pi^+\omega$  and  $B^0 \rightarrow \pi^0\omega$  decays, in a modified perturbative QCD approach. In this approach, we calculate non-factorizable and annihilation type contributions, in addition to the usual factorizable contributions. Our result is in agreement with the measured branching ratio of  $B^0/\bar{B}^0 \rightarrow \pi^\pm\rho^\mp$ ,  $B^+ \rightarrow \pi^+\rho^0$ ,  $\pi^+\omega$  by CLEO and BABAR collaboration. We also predict large CP asymmetries in these decays. These channels are useful to determine the CKM angle  $\phi_2$ .

PACS: 13.25.Hw, 11.10.Hi, 12.38.Bx,

---

\*Mailing address

# 1 Introduction

The rare decays of B mesons are getting more and more interesting, since they are useful for search of CP violation and sensitive to new physics. The recent measurement of  $B \rightarrow \pi\rho$  and  $\pi\omega$  decays by CLEO Collaboration [1] arouse more discussions on these decays [2]. The  $B \rightarrow \pi\rho$ ,  $\pi\omega$  decays which are helpful to the determination of Cabibbo-Kobayashi-Maskawa (CKM) unitarity triangle  $\phi_2$  have been studied in the factorization approach in detail [3, 4]. In this paper, we would like to study the  $B \rightarrow \pi\rho$  and  $\pi\omega$  decays in the modified perturbative QCD approach (PQCD), where we can calculate the non-factorizable contributions as corrections to the usual factorization approach.

In the  $B \rightarrow \pi\rho$ ,  $\pi\omega$  decays, the  $B$  meson is heavy, sitting at rest. It decays into two light mesons with large momenta. Therefore the light mesons are moving very fast in the rest frame of  $B$  meson. In this case, the short distance hard process dominates the decay amplitude. The soft final state interaction is not important, since there is not enough time for the pions exchanging soft gluons. This makes the perturbative QCD approach applicable. With the final light mesons moving very fast, there must be a hard gluon to kick the light spectator quark (almost at rest) in the  $B$  meson to form a fast moving pion. So the dominant diagram in this theoretical picture is that one hard gluon from the the spectator quark connecting with the other quarks in the four quark operator of the weak interaction. There are also soft gluon exchanges between quarks. Summing over those leading soft contributions gives a Sudakov form factor, which suppresses the soft contribution to be dominant. Therefore, it makes the PQCD reliable in calculating the non-leptonic decays. With the Sudakov resummation, we can include the leading double logarithms for all loop diagrams, in association with the soft contribution. Unlike the usual factorization approach, the hard part of the PQCD approach consists of six quarks rather than four. We thus call it six-quark operators or six-quark effective theory. Applying the six-quark effective theory to B meson decays, we need meson wave functions for the hadronization of quarks into mesons. All the soft dynamics are included in the meson wave functions.

In this paper, we calculate the  $B \rightarrow \pi$  and  $B \rightarrow \rho$  form factors, which are input paramters used in factorization approach. The form factor calculations can give severe restrictions to the input meson wave functions. We also calculate the non-factorizable contributions and the

annihilation type diagrams, which are difficult to calculate in the factorization approach. We found that this type of diagrams give dominant contributions to strong phases. The strong phase in this approach can also be calculated directly, without ambiguity. In the next section, we will briefly introduce our method of PQCD. In section 3, we perform the perturbative calculations for all the channels. And we give the numerical results and discussions in section 4. Finally section 5 is a short summary.

## 2 The Frame Work

The three scale PQCD factorization theorem has been developed for non-leptonic heavy meson decays [5]. The factorization formula is given by the typical expression,

$$C(t) \times H(t) \times \Phi(x) \times \exp \left[ -s(P, b) - 2 \int_{1/b}^t \frac{d\bar{\mu}}{\bar{\mu}} \gamma_q(\alpha_s(\bar{\mu})) \right], \quad (1)$$

where  $C(t)$  are the corresponding Wilson coefficients,  $\Phi(x)$  are the meson wave functions. And the quark anomalous dimension  $\gamma_q = -\alpha_s/\pi$  describes the evolution from scale  $t$  to  $1/b$ .

Non-leptonic heavy meson decays involve three scales: the W boson mass  $m_W$ , at which the matching condition of the effective Hamiltonian are defined, the typical scale  $t$  of a hard subamplitude, which reflects the dynamics of heavy quark decays, and the factorization scale  $1/b$ , with  $b$  the conjugate variable of parton transverse momenta. The dynamics below  $1/b$  scale is regarded as being completely nonperturbative, and can be parametrized into meson wave functions. Above the scale  $1/b$ , PQCD is reliable and radiative corrections produce two types of large logarithms:  $\ln(m_W/t)$  and  $\ln(tb)$ . The former are summed by renormalization group equations to give the leading logarithm evolution from  $m_W$  to  $t$  scale contained in the Wilson coefficients  $C(t)$ . While the latter are summed to give the evolution from  $t$  scale down to  $1/b$ , shown as the last factor in eq.(1).

There exist also double logarithms  $\ln^2(Pb)$  from the overlap of collinear and soft divergences,  $P$  being the dominant light-cone component of a meson momentum. The resummation of these double logarithms leads to a Sudakov form factor  $\exp[-s(P, b)]$ , which suppresses the long distance contributions in the large  $b$  region, and vanishes as  $b > 1/\Lambda_{QCD}$ . This factor improves the applicability of PQCD. For the detailed derivation of the Sudakov form factors, see ref.[6, 7].

Since all logarithm corrections have been summed by renormalization group equations, the above factorization formula does not depend on the renormalization scale  $\mu$ .

With all the large logarithms resummed, the remaining finite contributions are absorbed into a hard subamplitude  $H(t)$ . The  $H(t)$  are calculated perturbatively involving the four quark operators together with the spectator quark, connected by a hard gluon.

## 2.1 Wilson Coefficients

First we begin with the weak effective Hamiltonian  $H_{eff}$  for the  $\Delta B = 1$  transitions as

$$\mathcal{H}_{eff} = \frac{G_F}{\sqrt{2}} \left[ V_{ub} V_{ud}^* (C_1 O_1^u + C_2 O_2^u) - V_{tb} V_{td}^* \sum_{i=3}^{10} C_i O_i \right] . \quad (2)$$

We specify below the operators in  $\mathcal{H}_{eff}$  for  $b \rightarrow d$ :

$$\begin{aligned} O_1^u &= \bar{d}_\alpha \gamma^\mu L u_\beta \cdot \bar{u}_\beta \gamma_\mu L b_\alpha , & O_2^u &= \bar{d}_\alpha \gamma^\mu L u_\alpha \cdot \bar{u}_\beta \gamma_\mu L b_\beta , \\ O_3 &= \bar{d}_\alpha \gamma^\mu L b_\alpha \cdot \sum_{q'} \bar{q}'_\beta \gamma_\mu L q'_\beta , & O_4 &= \bar{d}_\alpha \gamma^\mu L b_\beta \cdot \sum_{q'} \bar{q}'_\beta \gamma_\mu L q'_\alpha , \\ O_5 &= \bar{d}_\alpha \gamma^\mu L b_\alpha \cdot \sum_{q'} \bar{q}'_\beta \gamma_\mu R q'_\beta , & O_6 &= \bar{d}_\alpha \gamma^\mu L b_\beta \cdot \sum_{q'} \bar{q}'_\beta \gamma_\mu R q'_\alpha , \\ O_7 &= \frac{3}{2} \bar{d}_\alpha \gamma^\mu L b_\alpha \cdot \sum_{q'} e_{q'} \bar{q}'_\beta \gamma_\mu R q'_\beta , & O_8 &= \frac{3}{2} \bar{d}_\alpha \gamma^\mu L b_\beta \cdot \sum_{q'} e_{q'} \bar{q}'_\beta \gamma_\mu R q'_\alpha , \\ O_9 &= \frac{3}{2} \bar{d}_\alpha \gamma^\mu L b_\alpha \cdot \sum_{q'} e_{q'} \bar{q}'_\beta \gamma_\mu L q'_\beta , & O_{10} &= \frac{3}{2} \bar{d}_\alpha \gamma^\mu L b_\beta \cdot \sum_{q'} e_{q'} \bar{q}'_\beta \gamma_\mu L q'_\alpha . \end{aligned} \quad (3)$$

Here  $\alpha$  and  $\beta$  are the  $SU(3)$  color indices;  $L$  and  $R$  are the left- and right-handed projection operators with  $L = (1 - \gamma_5)$ ,  $R = (1 + \gamma_5)$ . The sum over  $q'$  runs over the quark fields that are active at the scale  $\mu = O(m_b)$ , i.e.,  $(q' \epsilon \{u, d, s, c, b\})$ .

The PQCD approach works well for the leading twist approximation and leading double logarithm summation. For the Wilson coefficients, we will also use the leading logarithm summation for the QCD corrections, although the next-to-leading order calculations already exist in the literature [8]. This is the consistent way to cancel the explicit  $\mu$  dependence in the theoretical formulae.

If the scale  $m_b < t < m_W$ , then we evaluate the Wilson coefficients at  $t$  scale using leading logarithm running equations [8], in the appendix B of ref.[10]. In numerical calculations, we use  $\alpha_s = 4\pi/[\beta_1 \ln(t^2/\Lambda_{QCD}^{(5)})^2]$  which is the leading order expression with  $\Lambda_{QCD}^{(5)} = 193\text{MeV}$ , derived from  $\Lambda_{QCD}^{(4)} = 250\text{MeV}$ . Here  $\beta_1 = (33 - 2n_f)/12$ , with the appropriate number of active quarks  $n_f$ .  $n_f = 5$  when scale  $t$  is larger than  $m_b$ .

If the scale  $t < m_b$ , then we evaluate the Wilson coefficients at  $t$  scale using the formulae in appendix C of ref.[10] for four active quarks ( $n_f = 4$ ) (again in leading logarithm approximation).

## 2.2 Wave Functions

In the resummation procedures, the  $B$  meson is treated as a heavy-light system. The wave function is defined as

$$\Phi_B = \frac{1}{\sqrt{6}}(\not{p}_B + m_B)\gamma_5\phi_B(\mathbf{k}_1, \mathbf{k}_2), \quad (4)$$

where  $\phi_B(\mathbf{k}_1, \mathbf{k}_2)$  is the distribution function of the 4-momenta of the light quark ( $\mathbf{k}_1$ ) and  $b$  quark ( $\mathbf{k}_2$ ). To form a bound state of  $B$  meson, the condition  $\mathbf{k}_2 = \mathbf{p}_B - \mathbf{k}_1$  is required. So  $\phi_B$  is actually a function of  $\mathbf{k}_1$  only. Through out this paper, we use the light-cone coordinates to write the four momentum as  $(k_1^+, k_1^-, k_1^\perp)$ . In the next section, we will see that the hard part is always independent of one of the  $k_1^+$  and/or  $k_1^-$ , if we make some approximations. The  $B$  meson wave function is then the function of variable  $k_1^-$  (or  $k_1^+$ ) and  $k_1^\perp$ .

$$\phi_B(k_1^-, k_1^\perp) = \int dk_1^+ \phi(k_1^+, k_1^-, k_1^\perp). \quad (5)$$

The  $\pi$  meson is treated as a light-light system. At the  $B$  meson rest frame, pion is moving very fast, one of  $k_1^+$  or  $k_1^-$  is zero depends on the definition of the z axis.

$$\Phi_\pi = \frac{1}{\sqrt{6}}\gamma_5 \left[ \not{p}_\pi \phi_\pi^A(k^+, k^\perp) + m_0 \phi_\pi^P(k^+, k^\perp) \right], \quad (6)$$

where  $m_0 = m_\pi^2/(m_u + m_d)$ . This is a scale characterized by the Chiral perturbation theory. The  $\rho$  meson wave function is defined as

$$\Phi_\rho = \frac{1}{\sqrt{6}} \not{\epsilon} [\not{p}_\rho + m_\rho] \phi_\rho(k^+, k^\perp). \quad (7)$$

Here for simplicity, we choose the same distribution function  $\phi_\rho$  for both terms  $\not{p}_\rho$  and  $m_\rho$ . The latter term is the leading twist wave function, while the first term is subleading twist. In the calculations of next section, we will show that the higher twist contribution suppressed by  $m_\rho/m_B$ , is very small.

The transverse momentum  $k^\perp$  is usually conveniently converted to the  $b$  parameter by Fourier transformation. The initial conditions of  $\phi_i(x)$ ,  $i = B, \pi$ , are of nonperturbative origin,

satisfying the normalization

$$\int_0^1 \phi_i(x, b=0) dx = \frac{1}{2\sqrt{6}} f_i, \quad (8)$$

with  $f_i$  the meson decay constants.

### 3 Perturbative Calculations

In the previous section we have discussed the wave functions and Wilson coefficients of the factorization formula in eq.(1). In this section, we will calculate the hard part  $H(t)$ . This part involves the four quark operators and the necessary hard gluon connecting the four quark operator and the spectator quark. Since the final results are expressed as integrations of the distribution function variables, we will show the whole amplitude for each diagram including wave functions.

Similar to the  $B \rightarrow \pi\pi$  decays [10], there are 8 type diagrams contributing to the  $B \rightarrow \pi\rho$  decays, which are shown in Figure 1. Let's first calculate the usual factorizable diagrams (a) and (b). Operators  $O_1, O_2, O_3, O_4, O_9$ , and  $O_{10}$  are  $(V-A)(V-A)$  currents, the sum of their amplitudes is given as

$$\begin{aligned} F_e = & 8\sqrt{2}\pi C_F G_F f_\rho m_\rho m_B^2 (\epsilon \cdot p_\pi) \int_0^1 dx_1 dx_2 \int_0^\infty b_1 db_1 b_2 db_2 \phi_B(x_1, b_1) \\ & \left\{ \left[ (1+x_2)\phi_\pi^A(x_2, b_2) + (1-2x_2)\phi_\pi^P(x_2, b_2) r_\pi \right] \alpha_s(t_e^1) \right. \\ & h_e(x_1, x_2, b_1, b_2) \exp[-S_{ab}(t_e^1)] \\ & \left. + 2r_\pi \phi_\pi^P(x_2, b_2) \alpha_s(t_e^2) h_e(x_2, x_1, b_2, b_1) \exp[-S_{ab}(t_e^2)] \right\}, \end{aligned} \quad (9)$$

where  $r_\pi = m_0/m_B = m_\pi^2/[m_B(m_u + m_d)]$ ;  $C_F = 4/3$  is a color factor. The function  $h_e$  and the Sudakov factors  $S_{ab}$  are displayed in the appendix. The diagrams Fig.1(a)(b) are also the diagrams for the  $B \rightarrow \pi$  form factor  $F_1^{B \rightarrow \pi}$ . Therefore we can extract  $F_1^{B \rightarrow \pi}$  from eq.(9).

$$F_1^{B \rightarrow \pi}(q^2 = 0) = \frac{F_e}{2\sqrt{2}C_F G_F f_\rho m_\rho (\epsilon \cdot p_\pi)}. \quad (10)$$

The operators  $O_5, O_6, O_7$ , and  $O_8$  have a structure of  $(V-A)(V+A)$ . Unlike the  $B \rightarrow \pi\pi$  decays, the sum of their amplitudes is

$$F_e^P = 0. \quad (11)$$

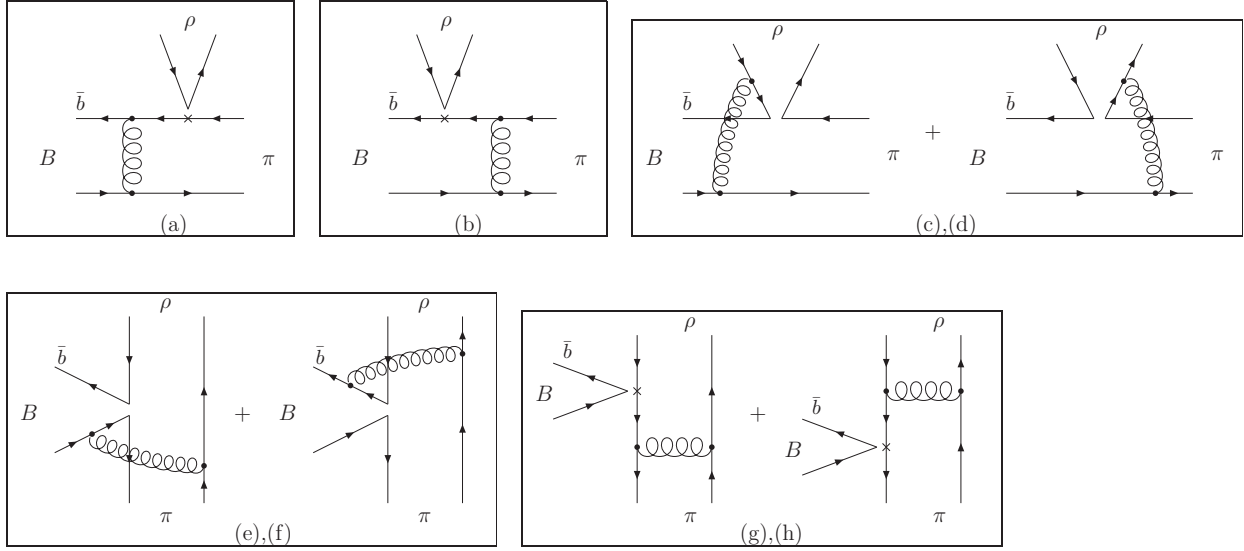


Figure 1: Diagrams contributing to the  $B \rightarrow \pi\rho$  decays (diagram (a) and (b) contribute to the  $B \rightarrow \pi$  form factor).

For the non-factorizable diagrams (c) and (d), all three meson wave functions are involved. The integration of  $b_3$  can be performed easily using  $\delta$  function  $\delta(b_3 - b_1)$ , leaving only integration of  $b_1$  and  $b_2$ . For the  $(V - A)(V - A)$  operators the result is

$$M_e = -\frac{32}{3}\sqrt{3}\pi C_F G_F m_\rho^2 m_B^2 (\epsilon \cdot p_\pi) \int_0^1 dx_1 dx_2 dx_3 \int_0^\infty b_1 db_1 b_2 db_2 \phi_B(x_1, b_1) x_2 \times \phi_\pi^A(x_2, b_1) \phi_\rho(x_3, b_2) h_d(x_1, x_2, x_3, b_1, b_2) \exp[-S_{cd}(t_d)] . \quad (12)$$

For the  $(V - A)(V + A)$  operators the formula are different,

$$M_e^P = -\frac{64}{3}\sqrt{3}\pi C_F G_F m_\rho^2 m_B^2 (\epsilon \cdot p_\pi) \int_0^1 dx_1 dx_2 dx_3 \int_0^\infty b_1 db_1 b_2 db_2 \phi_B(x_1, b_1) [x_3 + r_\pi(x_3 - x_2)] \times \phi_\pi^A(x_2, b_1) \phi_\rho(x_3, b_2) h_d(x_1, x_2, x_3, b_1, b_2) \exp[-S_{cd}(t_d)] . \quad (13)$$

Comparing with the expression of  $M_e$  in eq.(12), the  $(V - A)(V + A)$  type result  $M_e^P$  is suppressed by  $m_\rho/m_B$ .

For the non-factorizable annihilation diagrams (e) and (f), again all three wave functions are involved. The integration of  $b_3$  can be performed easily using  $\delta$  function  $\delta(b_3 - b_2)$ . Here we have two kind of contributions, which are different.  $M_a$  is contribution containing operator type  $(V - A)(V - A)$ , and  $M_a^P$  is contribution containing operator type  $(V - A)(V + A)$ .

$$M_a = \frac{32}{3}\sqrt{3}\pi C_F G_F m_\rho^2 m_B^2 (\epsilon \cdot p_\pi) \int_0^1 dx_1 dx_2 dx_3 \int_0^\infty b_1 db_1 b_2 db_2 \phi_B(x_1, b_1) \phi_\rho(x_3, b_2)$$

$$\times \left\{ [x_2 \phi_\pi^A(x_2, b_2) + r_\pi r_\rho(x_2 - x_3) \phi_\pi^P(x_2, b_2)] h_f^1(x_1, x_2, x_3, b_1, b_2) \exp[-S_{ef}(t_f^1)] \right. \quad (14)$$

$$\left. - [x_3 \phi_\pi^A(x_2, b_2) + r_\pi r_\rho(x_3 - x_2) \phi_\pi^P(x_2, b_2)] h_f^2(x_1, x_2, x_3, b_1, b_2) \exp[-S_{ef}(t_f^2)] \right\} ,$$

$$\begin{aligned} M_a^P = & -\frac{32}{3} \sqrt{3} \pi C_F G_F m_\rho m_0 m_B (\epsilon \cdot p_\pi) \int_0^1 dx_1 dx_2 dx_3 \int_0^\infty b_1 db_1 b_2 db_2 \phi_B(x_1, b_1) \\ & \times \left\{ [x_2 - r_\rho x_3] h_f^1(x_1, x_2, x_3, b_1, b_2) \exp[-S_{ef}(t_f^1)] \right. \\ & \left. + [2 - x_2 - r_\rho(2 - x_3)] h_f^2(x_1, x_2, x_3, b_1, b_2) \exp[-S_{ef}(t_f^2)] \right\} \phi_\pi^P(x_2, b_2) \phi_\rho(x_3, b_2). \end{aligned} \quad (15)$$

The factorizable annihilation diagrams (g) and (h) involve only  $\pi$  and  $\rho$  wave functions. There are also two kinds of decay amplitudes for these two diagrams.  $F_a$  is for  $(V - A)(V - A)$  type operators, and  $F_a^P$  is for  $(V - A)(V + A)$  type operators.

$$\begin{aligned} F_a = & 8\sqrt{2} C_F G_F \pi f_B m_\rho m_B^2 (\epsilon \cdot p_\pi) \int_0^1 dx_1 dx_2 \int_0^\infty b_1 db_1 b_2 db_2 \phi_\rho(x_2, b_2) \\ & \times \left\{ [x_2 \phi_\pi^A(x_1, b_1) - 2(1 - x_2) r_\pi r_\rho \phi_\pi^P(x_1, b_1)] \alpha_s(t_e^1) h_a(x_2, x_1, b_2, b_1) \exp[-S_{gh}(t_e^1)] \right. \\ & \left. - x_1 \phi_\pi^A(x_1, b_1) \alpha_s(t_e^2) h_a(x_1, x_2, b_1, b_2) \exp[-S_{gh}(t_e^2)] \right\}, \end{aligned} \quad (16)$$

$$\begin{aligned} F_a^P = & 16\sqrt{2} C_F G_F \pi f_B m_\rho m_B (\epsilon \cdot p_\pi) \int_0^1 dx_1 dx_2 \int_0^\infty b_1 db_1 b_2 db_2 \phi_\rho(x_2, b_2) \\ & \times \left\{ [2r_\pi \phi_\pi^P(x_1, b_1) - x_2 r_\rho \phi_\pi^A(x_1, b_1)] \alpha_s(t_e^1) h_a(x_2, x_1, b_2, b_1) \exp[-S_{gh}(t_e^1)] \right. \\ & \left. + x_2 r_\pi \phi_\pi^P(x_1, b_1) \alpha_s(t_e^2) h_a(x_1, x_2, b_1, b_2) \exp[-S_{gh}(t_e^2)] \right\}, \end{aligned} \quad (17)$$

In the above equations, we have used the assumption that  $x_1 \ll x_2, x_3$ . Since the light quark momentum fraction  $x_1$  in  $B$  meson is peaked at the small region, while quark momentum fraction  $x_2$  of pion is peaked around 0.5, this is not a bad approximation. The numerical results also show that this approximation makes very little difference in the final result. After using this approximation, all the diagrams are functions of  $k_1^- = x_1 m_B / \sqrt{2}$  of  $B$  meson only, independent of the variable of  $k_1^+$ . Therefore the integration of eq.(5) is performed safely. The scale  $t_i$ 's in the above equations are chosen as

$$t_e^1 = \max(\sqrt{x_2} m_B, 1/b_1, 1/b_2), \quad (18)$$

$$t_e^2 = \max(\sqrt{x_1} m_B, 1/b_1, 1/b_2), \quad (19)$$

$$t_d = \max(\sqrt{x_1 x_2} m_B, \sqrt{x_2 x_3} m_B, 1/b_1, 1/b_2),$$

$$t_f^1 = \max(\sqrt{x_2 x_3} m_B, 1/b_1, 1/b_2),$$

$$t_f^2 = \max(\sqrt{x_2 x_3} m_B, \sqrt{x_2 + x_3 - x_2 x_3} m_B, 1/b_1, 1/b_2). \quad (20)$$

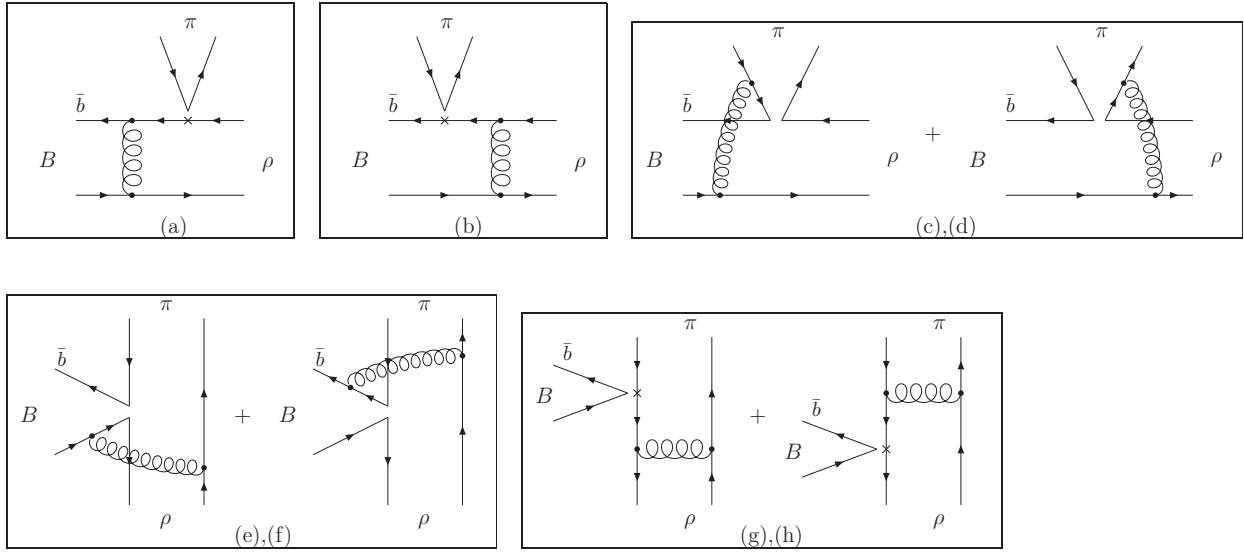


Figure 2: Diagrams contributing to the  $B \rightarrow \pi\rho$  decays (diagram (a) and (b) contribute to the  $B \rightarrow \rho$  form factor  $A_0^{B \rightarrow \rho}$ ).

If we exchange the  $\pi$  and  $\rho$  in Figure 1, the result will be different for some diagrams. Because this will switch the dominant contribution from  $B \rightarrow \pi$  form factor to  $B \rightarrow \rho$  form factor. The new diagrams are shown in Figure 2. Inserting  $(V - A)(V - A)$  operators, the corresponding amplitude for Figure 2(a) is

$$F_{e\rho} = 8\sqrt{2}\pi C_F G_F f_\pi m_\rho m_B^2 (\epsilon \cdot p_\pi) \int_0^1 dx_1 dx_2 \int_0^\infty b_1 db_1 b_2 db_2 \phi_B(x_1, b_1) \phi_\rho(x_2, b_2) \times [1 + x_2 + (1 - 2x_2)r_\rho] h_e(x_1, x_2, b_1, b_2) \exp[-S_{ab}(t_e^1)], \quad (21)$$

while the second diagram Figure 2(b) contributes zero. These two diagrams are also responsible for the calculation of  $B \rightarrow \rho$  form factors. The form factor relative to the  $B \rightarrow \pi\rho$  decays is  $A_0^{B \rightarrow \rho}$ , which can be extracted from eq.(21)

$$A_0^{B \rightarrow \rho}(q^2 = 0) = \frac{F_{e\rho}}{2\sqrt{2}C_F G_F f_\pi m_\rho (\epsilon \cdot p_\pi)}. \quad (22)$$

For  $(V - A)(V + A)$  operators, Figure 2(a) and 2(b) give

$$F_{e\rho}^P = -16\sqrt{2}\pi C_F G_F f_\pi m_\rho r_\pi m_B^2 (\epsilon \cdot p_\pi) \int_0^1 dx_1 dx_2 \int_0^\infty b_1 db_1 b_2 db_2 \phi_B(x_1, b_1) \times \phi_\rho(x_2, b_2) \left\{ (1 - r_\rho x_2) \alpha_s(t_e^1) h_e(x_1, x_2, b_1, b_2) \exp[-S_{ab}(t_e^1)] + x_1 \alpha_s(t_e^2) h_e(x_2, x_1, b_2, b_1) \exp[-S_{ab}(t_e^2)] \right\}, \quad (23)$$

For the nonfactorizable diagrams Figure 2(c) and 2(d) the result is

$$M_{e\rho} = -\frac{32}{3}\sqrt{3}\pi C_F G_F m_\rho m_B^2 (\epsilon \cdot p_\pi) \int_0^1 dx_1 dx_2 dx_3 \int_0^\infty b_1 db_1 b_2 db_2 \phi_B(x_1, b_1) \times x_2 (1 - 2r_\rho) \phi_\rho(x_2, b_2) \phi_\pi^A(x_3, b_1) h_d(x_1, x_2, x_3, b_1, b_2) \exp[-S_{cd}(t_d)]. \quad (24)$$

For the nonfactorizable annihilation diagrams (e) and (f), we have  $M_{a\rho}$  for  $(V - A)(V - A)$  operators and  $M_{a\rho}^P$  for  $(V - A)(V + A)$  operators.

$$M_{a\rho} = \frac{32}{3}\sqrt{3}\pi C_F G_F m_\rho m_B^2 (\epsilon \cdot p_\pi) \int_0^1 dx_1 dx_2 dx_3 \int_0^\infty b_1 db_1 b_2 db_2 \phi_B(x_1, b_1) \phi_\rho(x_2, b_2) \times \left\{ [x_2 \phi_\pi^A(x_3, b_2) + r_\pi r_\rho(x_2 - x_3) \phi_\pi^P(x_3, b_2)] h_f^1(x_1, x_2, x_3, b_1, b_2) \exp[-S_{ef}(t_f^1)] \right. \\ \left. - [x_3 \phi_\pi^A(x_3, b_2) + r_\pi r_\rho(x_3 - x_2) \phi_\pi^P(x_3, b_2)] h_f^2(x_1, x_2, x_3, b_1, b_2) \exp[-S_{ef}(t_f^2)] \right\}, \quad (25)$$

$$M_{a\rho}^P = M_a^P, \quad (26)$$

For the factorizable annihilation diagrams (g) and (h)

$$F_{a\rho} = -F_a, \quad (27)$$

$$F_{a\rho}^P = -F_a^P, \quad (28)$$

If the  $\rho$  meson replaced by  $\omega$  meson in Figure 1 and 2, the formulas will be the same, except replacing  $f_\rho$  by  $f_\omega$  and  $\phi_\rho$  replaced by  $\phi_\omega$ .

In the language of the above matrix elements for different diagrams eq.(9-28.), the decay amplitude for  $B^0 \rightarrow \pi^+ \rho^-$  can be written as

$$\mathcal{M}(B^0 \rightarrow \pi^+ \rho^-) = F_{e\rho} \left[ \xi_u \left( \frac{1}{3} C_1 + C_2 \right) - \xi_t \left( C_4 + \frac{1}{3} C_3 + C_{10} + \frac{1}{3} C_9 \right) \right] \\ - F_{e\rho}^P \xi_t \left[ C_6 + \frac{1}{3} C_5 + C_8 + \frac{1}{3} C_7 \right] \\ + M_{e\rho} [\xi_u C_1 - \xi_t (C_3 + C_9)] \\ + M_a \left[ \xi_u C_2 - \xi_t \left( C_4 - C_6 + \frac{1}{2} C_8 + C_{10} \right) \right] \\ - M_{a\rho} \xi_t \left[ C_3 + C_4 - C_6 - C_8 - \frac{1}{2} C_9 - \frac{1}{2} C_{10} \right] \\ - M_a^P \xi_t \left[ C_5 - \frac{1}{2} C_7 \right] + F_a \left[ \xi_u \left( C_1 + \frac{1}{3} C_2 \right) \right. \\ \left. - \xi_t \left( -\frac{1}{3} C_3 - C_4 - \frac{3}{2} C_7 - \frac{1}{2} C_8 + \frac{5}{3} C_9 + C_{10} \right) \right] \\ + F_a^P \xi_t \left[ \frac{1}{3} C_5 + C_6 - \frac{1}{6} C_7 - \frac{1}{2} C_8 \right]. \quad (29)$$

where  $\xi_u = V_{ub}^* V_{ud}$ ,  $\xi_t = V_{tb}^* V_{td}$ . The  $C'_i$ s should be calculated at the appropriate scale  $t$  using equations in the appendices of ref.[10]. The decay amplitude of the charge conjugate decay channel  $\bar{B}^0 \rightarrow \rho^+ \pi^-$  is the same as eq.(29) except replacing the CKM matrix elements  $\xi_u$  to  $\xi_u^*$  and  $\xi_t$  to  $\xi_t^*$  under the definition of charge conjugation  $C|B^0\rangle = -|\bar{B}^0\rangle$ .

$$\begin{aligned}
\mathcal{M}(B^0 \rightarrow \rho^+ \pi^-) = & F_e \left[ \xi_u \left( \frac{1}{3} C_1 + C_2 \right) - \xi_t \left( C_4 + \frac{1}{3} C_3 + C_{10} + \frac{1}{3} C_9 \right) \right] \\
& + M_e [\xi_u C_1 - \xi_t (C_3 + C_9)] - M_e^P \xi_t [C_5 + C_7] \\
& + M_{a\rho} \left[ \xi_u C_2 - \xi_t \left( C_4 - C_6 + \frac{1}{2} C_8 + C_{10} \right) \right] \\
& - M_a \xi_t \left[ C_3 + C_4 - C_6 - C_8 - \frac{1}{2} C_9 - \frac{1}{2} C_{10} \right] \\
& - M_a^P \xi_t \left[ C_5 - \frac{1}{2} C_7 \right] + F_a \left[ \xi_u \left( -C_1 - \frac{1}{3} C_2 \right) \right. \\
& \quad \left. - \xi_t \left( \frac{1}{3} C_3 + C_4 + \frac{3}{2} C_7 + \frac{1}{2} C_8 - \frac{5}{3} C_9 - C_{10} \right) \right] \\
& - F_a^P \xi_t \left[ \frac{1}{3} C_5 + C_6 - \frac{1}{6} C_7 - \frac{1}{2} C_8 \right]. \tag{30}
\end{aligned}$$

The decay amplitude for  $B^0 \rightarrow \pi^0 \rho^0$  can be written as

$$\begin{aligned}
-2\mathcal{M}(B^0 \rightarrow \pi^0 \rho^0) = & F_e \left[ \xi_u \left( C_1 + \frac{1}{3} C_2 \right) \right. \\
& \left. - \xi_t \left( -\frac{1}{3} C_3 - C_4 + \frac{3}{2} C_7 + \frac{1}{2} C_8 + \frac{5}{3} C_9 + C_{10} \right) \right] \\
& + F_{e\rho} \left[ \xi_u \left( C_1 + \frac{1}{3} C_2 \right) \right. \\
& \left. - \xi_t \left( -\frac{1}{3} C_3 - C_4 - \frac{3}{2} C_7 - \frac{1}{2} C_8 + \frac{5}{3} C_9 + C_{10} \right) \right] \\
& + F_{e\rho}^P \xi_t \left[ \frac{1}{3} C_5 + C_6 - \frac{1}{6} C_7 - \frac{1}{2} C_8 \right] \\
& + M_e \left[ \xi_u C_2 - \xi_t (-C_3 - \frac{3}{2} C_8 + \frac{1}{2} C_9 + \frac{3}{2} C_{10}) \right] \\
& + M_{e\rho} \left[ \xi_u C_2 - \xi_t (-C_3 + \frac{3}{2} C_8 + \frac{1}{2} C_9 + \frac{3}{2} C_{10}) \right] \\
& - (M_a + M_{a\rho}) [\xi_u C_2 \\
& \quad - \xi_t (C_3 + 2C_4 - 2C_6 - \frac{1}{2} C_8 - \frac{1}{2} C_9 + \frac{1}{2} C_{10})] \\
& + (M_e^P + 2M_a^P) \xi_t \left[ C_5 - \frac{1}{2} C_7 \right]. \tag{31}
\end{aligned}$$

The decay amplitude for  $B^+ \rightarrow \rho^+ \pi^0$  can be written as

$$\sqrt{2} \mathcal{M}(B^+ \rightarrow \rho^+ \pi^0) = (F_e + 2F_a) \left[ \xi_u \left( \frac{1}{3} C_1 + C_2 \right) - \xi_t \left( \frac{1}{3} C_3 + C_4 + C_{10} + \frac{1}{3} C_9 \right) \right]$$

$$\begin{aligned}
& + F_{e\rho} \left[ \xi_u \left( C_1 + \frac{1}{3} C_2 \right) - \xi_t \left( -\frac{1}{3} C_3 - C_4 - \frac{3}{2} C_7 - \frac{1}{2} C_8 + C_{10} + \frac{5}{3} C_9 \right) \right] \\
& - F_{e\rho}^P \xi_t \left[ -\frac{1}{3} C_5 - C_6 + \frac{1}{2} C_8 + \frac{1}{6} C_7 \right] \\
& + M_{e\rho} \left[ \xi_u C_2 - \xi_t (-C_3 + \frac{3}{2} C_8 + \frac{1}{2} C_9 + \frac{3}{2} C_{10}) \right] \\
& + (M_e + M_a - M_{a\rho}) [\xi_u C_1 - \xi_t (C_3 + C_9)] \\
& - M_e^P \xi_t [C_5 + C_7] - 2F_a^P \xi_t \left[ \frac{1}{3} C_5 + C_6 + \frac{1}{3} C_7 + C_8 \right]. \tag{32}
\end{aligned}$$

The decay amplitude for  $B^+ \rightarrow \pi^+ \rho^0$  can be written as

$$\begin{aligned}
\sqrt{2}\mathcal{M}(B^+ \rightarrow \pi^+ \rho^0) & = F_e \left[ \xi_u \left( C_1 + \frac{1}{3} C_2 \right) \right. \\
& \quad \left. - \xi_t \left( -\frac{1}{3} C_3 - C_4 + \frac{3}{2} C_7 + \frac{1}{2} C_8 + \frac{5}{3} C_9 + C_{10} \right) \right] \\
& + (F_{e\rho} - 2F_a) \left[ \xi_u \left( \frac{1}{3} C_1 + C_2 \right) - \xi_t \left( \frac{1}{3} C_3 + C_4 + \frac{1}{3} C_9 + C_{10} \right) \right] \\
& - (F_{e\rho}^P - 2F_a^P) \xi_t \left[ \frac{1}{3} C_5 + C_6 + \frac{1}{3} C_7 + C_8 \right] \\
& + M_e \left[ \xi_u C_2 - \xi_t (-C_3 - \frac{3}{2} C_8 + \frac{1}{2} C_9 + \frac{3}{2} C_{10}) \right] \\
& + (M_{e\rho} - M_a + M_{a\rho}) [\xi_u C_1 - \xi_t (C_3 + C_9)] \\
& + M_e^P \xi_t \left[ C_5 - \frac{1}{2} C_7 \right]. \tag{33}
\end{aligned}$$

From eq.(29-33), we can verify that the isospin relation

$$\begin{aligned}
\mathcal{M}(B^0 \rightarrow \pi^+ \rho^-) + \mathcal{M}(B^0 \rightarrow \pi^- \rho^+) - 2\mathcal{M}(B^0 \rightarrow \pi^0 \rho^0) & \tag{34} \\
= \sqrt{2}\mathcal{M}(B^+ \rightarrow \pi^0 \rho^+) + \sqrt{2}\mathcal{M}(B^+ \rightarrow \pi^+ \rho^0), &
\end{aligned}$$

holds exactly in our calculations.

The decay amplitude for  $B^+ \rightarrow \pi^+ \omega$  can also be written as expressions of the above  $F_i$  and  $M_i$ , but remember replacing  $f_\rho$  by  $f_\omega$  and  $\phi_\rho$  by  $\phi_\omega$ .

$$\begin{aligned}
\sqrt{2}\mathcal{M}(B^+ \rightarrow \pi^+ \omega) & = F_e \left[ \xi_u \left( C_1 + \frac{1}{3} C_2 \right) \right. \\
& \quad \left. - \xi_t \left( \frac{7}{3} C_3 + \frac{5}{3} C_4 + 2C_5 + \frac{2}{3} C_6 + \frac{1}{2} C_7 + \frac{1}{6} C_8 + \frac{1}{3} C_9 - \frac{1}{3} C_{10} \right) \right] \\
& + F_{e\rho} \left[ \xi_u \left( \frac{1}{3} C_1 + C_2 \right) - \xi_t \left( \frac{1}{3} C_3 + C_4 + \frac{1}{3} C_9 + C_{10} \right) \right] \\
& - F_{e\rho}^P \xi_t \left[ \frac{1}{3} C_5 + C_6 + \frac{1}{3} C_7 + C_8 \right]
\end{aligned}$$

$$\begin{aligned}
& + M_e \left[ \xi_u C_2 - \xi_t (C_3 + 2C_4 - 2C_6 - \frac{1}{2}C_8 - \frac{1}{2}C_9 + \frac{1}{2}C_{10}) \right] \\
& + (M_{e\rho} + M_a + M_{a\rho}) [\xi_u C_1 - \xi_t (C_3 + C_9)] \\
& - (M_a^P + M_{a\rho}^P) \xi_t [C_5 + C_7] - M_e^P \xi_t \left[ C_5 - \frac{1}{2}C_7 \right]. \tag{35}
\end{aligned}$$

The decay amplitude for  $B^0 \rightarrow \pi^0 \omega$  can be written as

$$\begin{aligned}
2\mathcal{M}(B^0 \rightarrow \pi^0 \omega) = & F_e \left[ \xi_u \left( -C_1 - \frac{1}{3}C_2 \right) \right. \\
& - \xi_t \left( -\frac{7}{3}C_3 - \frac{5}{3}C_4 - 2C_5 - \frac{2}{3}C_6 - \frac{1}{2}C_7 - \frac{1}{6}C_8 - \frac{1}{3}C_9 + \frac{1}{3}C_{10} \right) \\
& + F_{e\rho} \left[ \xi_u \left( C_1 + \frac{1}{3}C_2 \right) \right. \\
& - \xi_t \left( -\frac{1}{3}C_3 - C_4 - \frac{3}{2}C_7 - \frac{1}{2}C_8 + \frac{5}{3}C_9 + C_{10} \right) \\
& + F_{e\rho}^P \xi_t \left[ C_6 + \frac{1}{3}C_5 - \frac{1}{6}C_7 - \frac{1}{2}C_8 \right] \\
& + M_e \left[ -\xi_u C_2 - \xi_t (-C_3 - 2C_4 + 2C_6 + \frac{1}{2}C_8 + \frac{1}{2}C_9 - \frac{1}{2}C_{10}) \right] \\
& + M_{e\rho} \left[ \xi_u C_2 - \xi_t (-C_3 + \frac{3}{2}C_8 + \frac{1}{2}C_9 + \frac{3}{2}C_{10}) \right] \\
& + (M_a + M_{a\rho}) \left[ \xi_u C_2 - \xi_t \left( -C_3 - \frac{3}{2}C_8 + \frac{1}{2}C_9 + \frac{3}{2}C_{10} \right) \right] \\
& + (M_e^P + 2M_a^P) \xi_t \left[ C_5 - \frac{1}{2}C_7 \right]. \tag{36}
\end{aligned}$$

## 4 Numerical calculations and discussions of Results

In the numerical calculations we use

$$\Lambda_{\overline{\text{MS}}}^{(f=4)} = 0.25 \text{GeV}, f_\pi = 130 \text{MeV}, f_B = 210 \text{MeV},$$

$$m_0 = 1 \text{GeV}, f_\rho = 220 \text{MeV}, f_\omega = 220 \text{MeV},$$

$$M_B = 5.2792 \text{GeV}, M_W = 80.41 \text{GeV}.$$

For the  $\pi$  wave function, we neglect the  $b$  dependence part, which is not important in numerical analysis. We use the same distribution function for the axial vector part as  $B \rightarrow \pi\pi$ , and  $B \rightarrow \pi K$  decays [10, 11].

$$\phi_\pi^A(x) = \frac{3}{\sqrt{6}} f_\pi x (1-x) \left[ 1 + 0.8 \{ 5(1-2x)^2 - 1 \} \right]. \tag{37}$$

The subleading twist wave function  $\phi_\pi^P$  is chosen as

$$\phi_\pi^P(x) = \frac{15}{\sqrt{6}} f_\pi x^2 (1-x)^2, \quad (38)$$

which can further suppress the contribution from the higher twist wave functions.

In  $B \rightarrow \pi\rho$  decays, it is the longitudinal polarization of the  $\rho$  meson contribute to the decay amplitude. Therefore we choose the wave function of  $\rho$  meson similar to the pion case in eq.(37)

$$\phi_\rho(x) = \frac{3}{\sqrt{6}} f_\rho x (1-x) \left[ 1 + \{5(1-2x)^2 - 1\} \right]. \quad (39)$$

For  $B$  meson, the wave function is chosen as

$$\phi_B(x, b_1) = \frac{N_B}{2\sqrt{6}} f_B x^2 (1-x)^2 \exp \left[ -\frac{M_B^2 x^2}{2\omega_{b1}^2} - \frac{1}{2} (\omega_{b2} b_1)^2 \right], \quad (40)$$

with  $\omega_{b1} = 0.28$  GeV,  $\omega_{b2} = 0.4$  GeV.  $N_B = 6372.69$  is a normalization factor. We choose a little smaller  $m_0$  and  $\omega_{b1}$  than that used in  $B \rightarrow \pi\pi$  decays [10]. These changes make the  $B \rightarrow \rho$  form factor a little larger than the  $B \rightarrow \pi$  form factor. This set of parameters only raise the  $B^0 \rightarrow \pi^+ \pi^-$  branching ratios around 20%. This is still in good agreement with the current experimental measurement [13]. And we will see later that, this set of parameters will give good results of  $B \rightarrow \pi\rho$  and  $\pi\omega$  decays. With the above chosen wave functions, we get the corresponding form factors at zero momentum transfer are:

$$F_0^{B \rightarrow \pi} = 0.31, \quad A_0^{B \rightarrow \rho} = 0.36.$$

They are close to the light cone QCD sum rule results [14].

The CKM parameters we used here are

$$\begin{aligned} |V_{ud}| &= 0.9740 \pm 0.0010 & |V_{ub}/V_{cb}| &= 0.08 \pm 0.02 \\ |V_{cb}| &= 0.0395 \pm 0.0017 & |V_{tb}^* V_{td}| &= 0.0084 \pm 0.0018. \end{aligned} \quad (41)$$

We leave the CKM angle  $\phi_2$  as a free parameter.  $\phi_2$ 's definition is

$$\phi_2 = \arg \left[ -\frac{V_{td} V_{tb}^*}{V_{ud} V_{ub}^*} \right]. \quad (42)$$

In this parameterization, the decay amplitude of  $B \rightarrow \pi\rho$  can be written as

$$\begin{aligned} \mathcal{M} &= V_{ub}^* V_{ud} T - V_{tb}^* V_{td} P \\ &= V_{ub}^* V_{ud} T \left[ 1 + z e^{i(\phi_2 + \delta)} \right], \end{aligned} \quad (43)$$

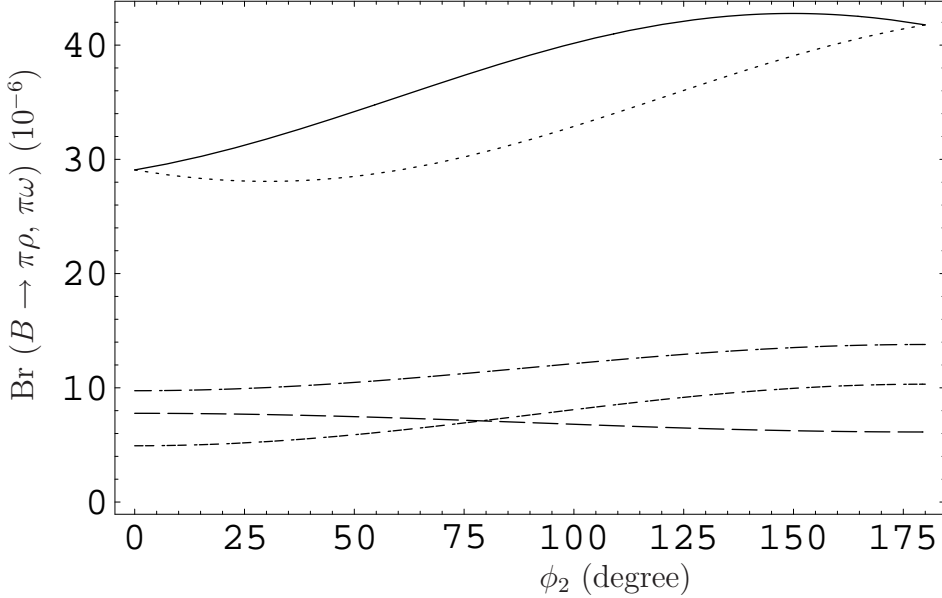


Figure 3: Branching ratios ( $10^{-6}$ ) of  $B^0/\bar{B}^0 \rightarrow \pi^+\rho^-$  (solid line),  $B^0/\bar{B}^0 \rightarrow \rho^+\pi^-$  (dotted line),  $B^+ \rightarrow \pi^+\rho^0$  (dashed line),  $B^+ \rightarrow \rho^+\pi^0$  (dash-dotted line), and  $B^+ \rightarrow \pi^+\omega$  (dash-dotted-dotted line), as a function of CKM angle  $\phi_2$ .

where  $z = \left| \frac{V_{tb}^* V_{td}}{V_{ub}^* V_{ud}} \right| \left| \frac{P}{T} \right|$ , and  $\delta$  is the relative strong phase between tree (T) diagrams and penguin diagrams (P).  $z$  and  $\delta$  can be calculated from PQCD. The corresponding charge conjugate decay mode is then

$$\begin{aligned} \bar{\mathcal{M}} &= V_{ub} V_{ud}^* T - V_{tb} V_{td}^* P \\ &= V_{ub} V_{ud}^* T \left[ 1 + z e^{i(-\phi_2 + \delta)} \right]. \end{aligned} \quad (44)$$

Therefore the averaged branching ratio for  $B \rightarrow \pi\rho$  is

$$\begin{aligned} Br &= (|\mathcal{M}|^2 + |\bar{\mathcal{M}}|^2)/2 \\ &= |V_{ub} V_{ud}^* T|^2 \left[ 1 + 2z \cos \phi_2 \cos \delta + z^2 \right], \end{aligned} \quad (45)$$

where  $z = \left| \frac{V_{tb} V_{td}^*}{V_{ub} V_{ud}^*} \right| \left| \frac{P}{T} \right|$ . Eq.(45) shows that the averaged branching ratio is a function of  $\cos \phi_2$ . This gives potential method to determine the CKM angle  $\phi_2$  by measuring only non-leptonic decay branching ratios.

There are four decay channels of  $B^0/\bar{B}^0 \rightarrow \pi^+\rho^-$ ,  $B^0/\bar{B}^0 \rightarrow \rho^+\pi^-$ . Due to  $B\bar{B}$  mixing, it is very difficult to distinguish  $B^0$  from  $\bar{B}^0$ . But it is very easy to identify the final states. Therefore we sum up  $B^0/\bar{B}^0 \rightarrow \pi^+\rho^-$  as one channel, and  $B^0/\bar{B}^0 \rightarrow \rho^+\pi^-$  as another, although

the summed up channels are not charge conjugate states. We show the branching ratio of  $B^0/\bar{B}^0 \rightarrow \pi^+\rho^-$ ,  $B^0/\bar{B}^0 \rightarrow \rho^+\pi^-$ ,  $B^+ \rightarrow \pi^+\rho^0$ ,  $B^+ \rightarrow \rho^+\pi^0$ , and  $B^+ \rightarrow \pi^+\omega$  decays as a function of  $\phi_2$  in Figure 3. The branching ratio of  $B^0/\bar{B}^0 \rightarrow \pi^+\rho^-$  is a little larger than that of  $B^0/\bar{B}^0 \rightarrow \pi^-\rho^+$  decays. Each of them is a sum of two decay channels. They are all larger when  $\phi_2$  is larger. The average of the two is in agreement with the the recently measured branching ratios by CLEO [1] and BABAR [15]

$$\text{Br}(B^0 \rightarrow \pi^+\rho^- + \pi^-\rho^+) = 27.6^{+8.4}_{-7.4} \pm 4.2 \times 10^{-6}, \quad \text{CLEO} \quad (46)$$

$$\text{Br}(B^0 \rightarrow \pi^+\rho^- + \pi^-\rho^+) = 49 \pm 13^{+6}_{-5} \times 10^{-6}, \quad \text{BABAR} \quad (47)$$

There are still large uncertainties in the experimental results. Therefore it is still early to fully determine the input parameters and to tell the CKM angle  $\phi_2$  from experiments.

The branching ratios of  $B^+ \rightarrow \pi^+\rho^0$  and  $B^+ \rightarrow \pi^+\omega$  have little dependence on  $\phi_2$ . They are a little smaller than the CLEO measurement [1] showed below, but still within experimental error-bars.

$$\text{Br}(B^+ \rightarrow \pi^+\rho^0) = 10.4^{+3.3}_{-3.4} \pm 2.1 \times 10^{-6}. \quad (48)$$

$$\text{Br}(B^+ \rightarrow \pi^+\omega) = 11.3^{+3.3}_{-2.9} \pm 1.4 \times 10^{-6}. \quad (49)$$

The averaged branching ratios of  $B^0 \rightarrow \pi^0\rho^0$  and  $\pi^0\omega$  are shown in Fig.4. They also have a large dependence on  $\phi_2$ . The behavior of them is quite different, due to the different isospin of  $\rho^0$  and  $\omega$ . But their branching ratios are rather small around  $10^{-7}$ . They can not be measured in the current running B factories.

Using eq.(43-44), we can derive the direct CP violating parameter as

$$\begin{aligned} A_{CP}^{dir} &= \frac{|\mathcal{M}|^2 - |\overline{\mathcal{M}}|^2}{|\mathcal{M}|^2 + |\overline{\mathcal{M}}|^2} \\ &= \frac{2 \sin \phi_2 \sin \delta}{1 + 2z \cos \phi_2 \cos \delta + z^2}. \end{aligned} \quad (50)$$

Unsurprisingly, it is a function of  $\cos \phi_2$  and  $\sin \phi_2$ . They are calculable in our PQCD approach. The direct CP violation parameters as a function of  $\phi_2$  are shown in figure 5. The direct CP violation parameter of  $B^+ \rightarrow \pi^+\rho^0$  and  $B^0 \rightarrow \pi^0\rho^0$  are positive and very large. While the direct CP violation parameter of  $B^+ \rightarrow \rho^+\pi^0$  and  $B^0 \rightarrow \pi^0\omega$  are negative and very large. The

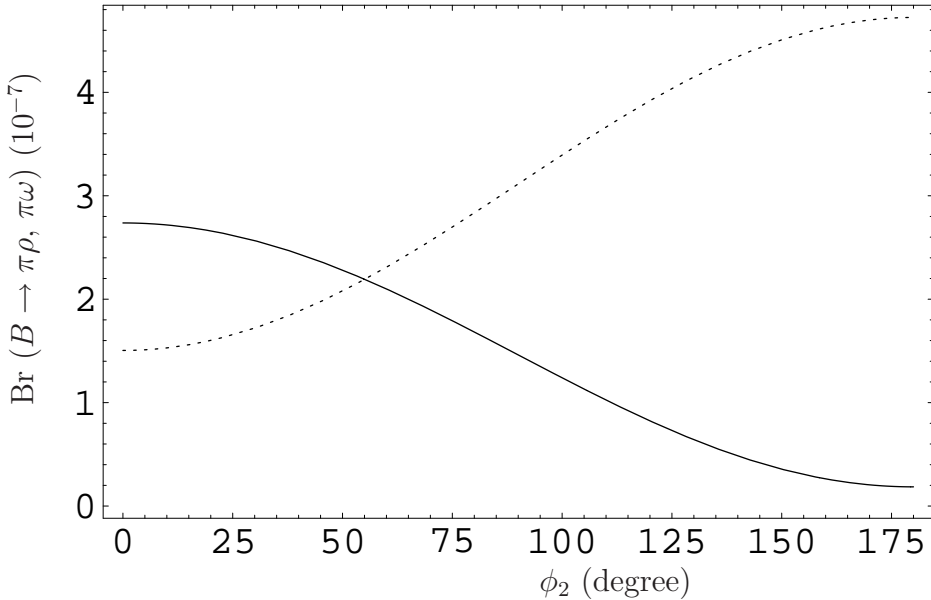


Figure 4: Branching ratios ( $10^{-7}$ ) of  $B^0 \rightarrow \pi^0 \rho^0$  (solid line),  $B^0 \rightarrow \pi^0 \omega$  (dotted line), as a function of CKM angle  $\phi_2$ .

large strong phase required by the large direct CP asymmetry is from the non-factorizable and annihilation type diagrams, especially the annihilation diagrams. This is the different situation in Factorization approach where the main contribution comes from BSS mechanism [16] and the annihilation diagram has been selected [9]. The direct CP violation of  $B^+ \rightarrow \pi^+ \omega$  is rather small, since the annihilation diagram contributions in this decay is almost canceled out in eq.(35). The preliminary measurement of CELO shows a large CP asymmetry for this decay [17]

$$A_{CP}(B^+ \rightarrow \pi^+ \omega) = 34 \pm 25\%. \quad (51)$$

Although the sign of CP is in agreement with our prediction, the central value is too large. If the result of central value remains in future experiments, we may expect new physics contributions.

For the neutral  $B^0$  decays, there is more complication from the  $B^0 \overline{B^0}$  mixing. The CP asymmetry is time dependent [9]:

$$A_{CP}(t) \simeq A_{CP}^{dir} \cos(\Delta m t) + a_{\epsilon+\epsilon'} \sin(\Delta m t), \quad (52)$$

where  $\Delta m$  is the mass difference of the two mass eigenstates of neutral  $B$  meson. The direct CP violation parameter  $A_{CP}^{dir}$  has already been defined in eq.(50). While the mixing-related CP

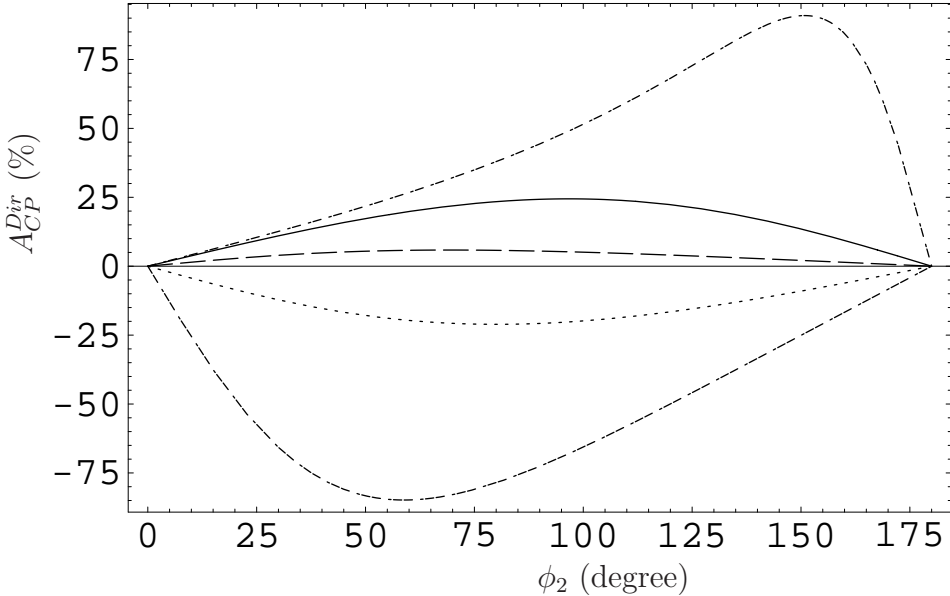


Figure 5: Direct CP violation parameters of  $B^+ \rightarrow \pi^+ \rho^0$  (solid line),  $B^+ \rightarrow \rho^+ \pi^0$  (dotted line),  $B^+ \rightarrow \pi^+ \omega$  (dashed line),  $B^0 \rightarrow \rho^0 \pi^0$  (dash-dotted line),  $B^0 \rightarrow \pi^0 \omega$  (dash-dotted-dotted line), as a function of CKM angle  $\phi_2$ .

violation parameter is defined as

$$a_{\epsilon+\epsilon'} = \frac{-2\text{Im}(\lambda_{CP})}{1 + |\lambda_{CP}|^2}, \quad (53)$$

where

$$\lambda_{CP} = \frac{V_{tb}^* V_{td} \langle f | H_{eff} | \bar{B}^0 \rangle}{V_{tb} V_{td}^* \langle f | H_{eff} | B^0 \rangle}. \quad (54)$$

Using equations (43,44), we can derive as

$$\lambda_{CP} = e^{2i\phi_2} \frac{1 + ze^{i(\delta-\phi_2)}}{1 + ze^{i(\delta+\phi_2)}}. \quad (55)$$

$\lambda_{CP}$  and  $a_{\epsilon+\epsilon'}$  are functions of CKM angle  $\phi_2$  only. Therefore, the CP asymmetry of  $B \rightarrow \pi \rho$  and  $\pi \omega$  decays can measure the CKM angle  $\phi_2$ , even if for the neutral B decays including the  $B\bar{B}$  mixing effect.

If we integrate the time variable  $t$ , we will get the total CP asymmetry as

$$A_{CP} = \frac{1}{1+x^2} A_{CP}^{dir} + \frac{x}{1+x^2} a_{\epsilon+\epsilon'}, \quad (56)$$

with  $x = \Delta m/\Gamma \simeq 0.723$  for the  $B^0 - \bar{B}^0$  mixing in SM [12]. The total CP asymmetries of  $B^0 \rightarrow \pi^0 \rho^0$ ,  $\pi^0 \omega$  are shown in Figure 6. Although the CP asymmetries are large, but it is still difficult to measure for experiments, since their branching ratios are small around  $10^{-7}$ .

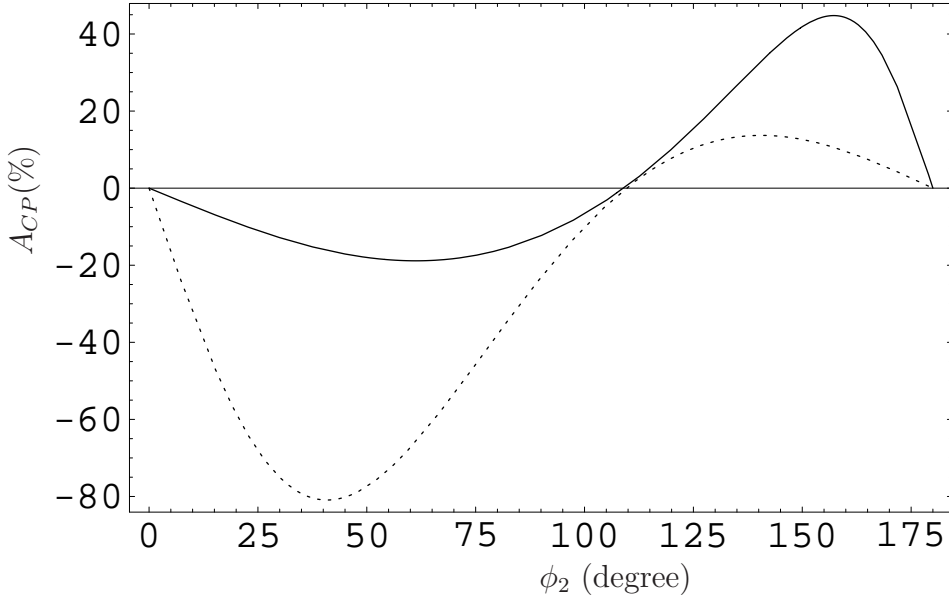


Figure 6: Total CP asymmetries of  $B^0 \rightarrow \pi^0 \rho^0$  (solid line), and  $B^0 \rightarrow \pi^0 \omega$  (dotted line), as a function of CKM angle  $\phi_2$ .

The CP asymmetries of  $B^0/\bar{B}^0 \rightarrow \pi^\pm \rho^\mp$  are very complicated. Here one studies the four time-dependent decay widths for  $B^0(t) \rightarrow \pi^+ \rho^-$ ,  $\bar{B}^0(t) \rightarrow \pi^- \rho^+$ ,  $B^0(t) \rightarrow \pi^- \rho^+$  and  $\bar{B}^0(t) \rightarrow \pi^+ \rho^-$  [18, 19, 20]. These time-dependent widths can be expressed by four basic matrix elements

$$\begin{aligned} g &= \langle \pi^+ \rho^- | H_{eff} | B^0 \rangle, & h &= \langle \pi^+ \rho^- | H_{eff} | \bar{B}^0 \rangle, \\ \bar{g} &= \langle \pi^- \rho^+ | H_{eff} | \bar{B}^0 \rangle, & \bar{h} &= \langle \pi^- \rho^+ | H_{eff} | B^0 \rangle, \end{aligned} \quad (57)$$

which determine the decay matrix elements of  $B^0 \rightarrow \pi^+ \rho^-$  &  $\pi^- \rho^+$  and of  $\bar{B}^0 \rightarrow \pi^- \rho^+$  &  $\pi^+ \rho^-$  at  $t = 0$ . The matrix elements  $g$  and  $\bar{h}$  are given in eq.(29,30). The matrix elements  $h$  and  $\bar{g}$  are obtained from  $\bar{h}$  and  $g$  by changing the signs of the weak phases contained in the products of the CKM matrix elements. We also need to know the CP-violating parameter coming from the  $B^0$  -  $\bar{B}^0$  mixing. Defining:

$$\begin{aligned} B_1 &= p|B^0\rangle + q|\bar{B}^0\rangle, \\ B_2 &= p|B^0\rangle - q|\bar{B}^0\rangle, \end{aligned} \quad (58)$$

with  $|p|^2 + |q|^2 = 1$  and  $q/p = \sqrt{H_{21}/H_{12}}$ , with  $H_{ij} = M_{ij} - i/2\Gamma_{ij}$  representing the  $|\Delta B| = 2$  and  $\Delta Q = 0$  Hamiltonian. For the decays of  $B^0$  and  $\bar{B}^0$ , we use,

$$\frac{q}{p} = \frac{V_{tb}^* V_{td}}{V_{tb} V_{td}^*} = e^{-2i\phi_1}. \quad (59)$$

So,  $|q/p| = 1$ , and this ratio has only a phase given by  $-2\phi_1$ . Then, the four time-dependent widths are given by the following formulae (we follow the notation of [20]):

$$\begin{aligned}\Gamma(B^0(t) \rightarrow \pi^+ \rho^-) &= e^{-\Gamma t} \frac{1}{2} (|g|^2 + |h|^2) \{1 + a_{\epsilon'} \cos \Delta m t + a_{\epsilon+\epsilon'} \sin \Delta m t\}, \\ \Gamma(\bar{B}^0(t) \rightarrow \pi^- \rho^+) &= e^{-\Gamma t} \frac{1}{2} (|\bar{g}|^2 + |\bar{h}|^2) \{1 - a_{\bar{\epsilon}'} \cos \Delta m t - a_{\epsilon+\bar{\epsilon}'} \sin \Delta m t\}, \\ \Gamma(B^0(t) \rightarrow \pi^- \rho^+) &= e^{-\Gamma t} \frac{1}{2} (|\bar{g}|^2 + |\bar{h}|^2) \{1 + a_{\bar{\epsilon}'} \cos \Delta m t + a_{\epsilon+\bar{\epsilon}'} \sin \Delta m t\}, \\ \Gamma(\bar{B}^0(t) \rightarrow \pi^+ \rho^-) &= e^{-\Gamma t} \frac{1}{2} (|g|^2 + |h|^2) \{1 - a_{\epsilon'} \cos \Delta m t - a_{\epsilon+\epsilon'} \sin \Delta m t\},\end{aligned}\quad (60)$$

where

$$\begin{aligned}a_{\epsilon'} &= \frac{|g|^2 - |h|^2}{|g|^2 + |h|^2}, & a_{\epsilon+\epsilon'} &= \frac{-2\text{Im}(\frac{q_h}{p_g})}{1 + |h/g|^2}, \\ a_{\bar{\epsilon}'} &= \frac{|\bar{h}|^2 - |\bar{g}|^2}{|\bar{h}|^2 + |\bar{g}|^2}, & a_{\epsilon+\bar{\epsilon}'} &= \frac{-2\text{Im}(\frac{q_{\bar{g}}}{p_{\bar{h}}})}{1 + |\bar{g}/\bar{h}|^2}.\end{aligned}\quad (61)$$

We calculate the above four CP violation parameters related to  $B^0/\bar{B}^0 \rightarrow \pi^\pm \rho^\mp$  decays in PQCD. The results are shown in Fig.7 as a function of  $\phi_2$ . Comparing the results with the factorization approach [9], we found that our predicted size of  $a'_\epsilon$  and  $a_{\bar{\epsilon}'}$  are smaller while  $a_{\epsilon+\epsilon'}$  and  $a_{\epsilon+\bar{\epsilon}'}$  are larger. By measuring the time-dependent spectrum of the decay rates of  $B^0$  and  $\bar{B}^0$ , one can find the coefficients of the two functions  $\cos \Delta m t$  and  $\sin \Delta m t$  in eq.(60) and extract the quantities  $a_{\epsilon'}$ ,  $a_{\epsilon+\epsilon'}$ ,  $a_{\bar{\epsilon}'}$ , and  $a_{\epsilon+\bar{\epsilon}'}$ . Using these experimental results, we can tell the size of CKM angle  $\phi_2$  from Fig.7.

## 5 Summary

We calculate the  $B^0 \rightarrow \pi^+ \rho^-$ ,  $B^0 \rightarrow \rho^+ \pi^-$ ,  $B^+ \rightarrow \rho^+ \pi^0$ ,  $B^+ \rightarrow \pi^+ \rho^0$ ,  $B^0 \rightarrow \pi^0 \rho^0$ ,  $B^+ \rightarrow \pi^+ \omega$  and  $B^0 \rightarrow \pi^0 \omega$  decays, together with their charge conjugate modes, in a modified perturbative QCD approach. We calculate the  $B \rightarrow \pi$  and  $B \rightarrow \rho$  form factors, which are in agreement with the QCD sum rule calculations. In addition to the usual factorization contributions, we also calculate the non-factorizable and annihilation diagrams. Although they are subleading contributions in the branching ratios of these decays, they are not negligible. Furthermore these diagrams provide the necessary strong phases required by the direct CP asymmetry measurement.

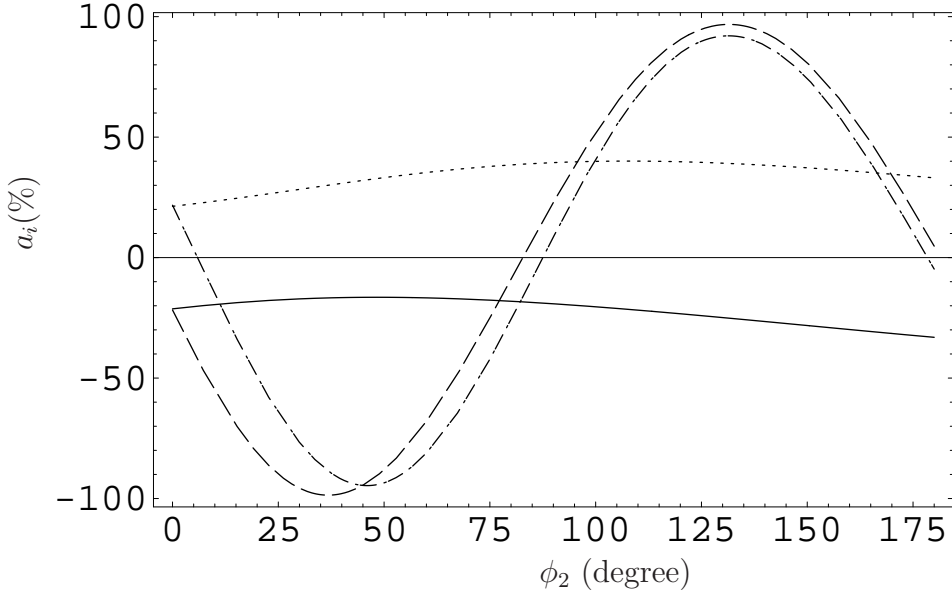


Figure 7: CP violation parameters of  $B^0/\bar{B}^0 \rightarrow \pi^\pm \rho^\mp$  decays:  $a'_\epsilon$  (solid line),  $a'_{\bar{\epsilon}}$  (dotted line),  $a_{\epsilon+\epsilon'}$  (dashed line) and  $a_{\epsilon+\bar{\epsilon}'}$  (dash-dotted line) as a function of CKM angle  $\phi_2$ .

Our calculation gives the right branching ratios, which agrees well with the CLEO and BABAR measurements. We also predict large direct CP asymmetries in  $B^+ \rightarrow \rho^+ \pi^0$  and  $B^+ \rightarrow \pi^+ \rho^0$  decays. Including the  $B\bar{B}$  mixing effect, the CP asymmetries of  $B^0 \rightarrow \pi^0 \omega$  and  $B^0 \rightarrow \pi^0 \rho^0$  are very large, but their branching ratios are small in SM. The CP asymmetry parameters of  $B^0 \rightarrow \pi^+ \rho^-$ ,  $B^0 \rightarrow \rho^+ \pi^-$  decays require the time dependent measurement of branching ratios.

## Acknowledgments

We thank our PQCD group members: Y.Y. Keum, E. Kou, T. Kurimoto, H.N. Li, T. Morozumi, A.I. Sanda, N. Sinha, R. Sinha, K. Ukai and T. Yoshikawa for helpful discussions. This work was supported by the Grant-in-Aid for Scientific Research on Priority Areas (Physics of CP violation). C.D. L. and M.Z. Y. thanks JSPS for support.

## A Related functions defined in the text

We show here the function  $h_i$ 's, coming from the Fourier transform of  $H^{(0)}$ ,

$$\begin{aligned} h_e(x_1, x_2, b_1, b_2) &= K_0(\sqrt{x_1 x_2} m_B b_1) [\theta(b_1 - b_2) K_0(\sqrt{x_2} m_B b_1) I_0(\sqrt{x_2} m_B b_2) \\ &\quad + \theta(b_2 - b_1) K_0(\sqrt{x_2} m_B b_2) I_0(\sqrt{x_2} m_B b_1)] \end{aligned} \quad (62)$$

$$\begin{aligned} h_d(x_1, x_2, x_3, b_1, b_2) &= \alpha_s(t_d) K_0(-i\sqrt{x_2 x_3} m_B b_2) \\ &\quad \times [\theta(b_1 - b_2) K_0(\sqrt{x_1 x_2} m_B b_1) I_0(\sqrt{x_1 x_2} m_B b_2) \\ &\quad + \theta(b_2 - b_1) K_0(\sqrt{x_1 x_2} m_B b_2) I_0(\sqrt{x_1 x_2} m_B b_1)] \end{aligned} \quad (63)$$

$$\begin{aligned} h_f^1(x_1, x_2, x_3, b_1, b_2) &= K_0(-i\sqrt{x_2 x_3} m_B b_1) \alpha_s(t_f^1) \\ &\quad \times [\theta(b_1 - b_2) K_0(-i\sqrt{x_2 x_3} m_B b_1) J_0(\sqrt{x_2 x_3} m_B b_2) \\ &\quad + \theta(b_2 - b_1) K_0(-i\sqrt{x_2 x_3} m_B b_2) J_0(\sqrt{x_2 x_3} m_B b_1)] \end{aligned} \quad (64)$$

$$\begin{aligned} h_f^2(x_1, x_2, x_3, b_1, b_2) &= K_0(\sqrt{x_2 + x_3 - x_2 x_3} m_B b_1) \alpha_s(t_f^2) \\ &\quad \times [\theta(b_1 - b_2) K_0(-i\sqrt{x_2 x_3} m_B b_1) J_0(\sqrt{x_2 x_3} m_B b_2) \\ &\quad + \theta(b_2 - b_1) K_0(-i\sqrt{x_2 x_3} m_B b_2) J_0(\sqrt{x_2 x_3} m_B b_1)] \end{aligned} \quad (65)$$

$$\begin{aligned} h_a(x_1, x_2, b_1, b_2) &= K_0(-i\sqrt{x_1 x_2} m_B b_2) \\ &\quad \times [\theta(b_1 - b_2) K_0(-i\sqrt{x_1} m_B b_1) J_0(\sqrt{x_1} m_B b_2) \\ &\quad + \theta(b_2 - b_1) K_0(-i\sqrt{x_1} m_B b_2) J_0(\sqrt{x_1} m_B b_1)], \end{aligned} \quad (66)$$

where  $J_0$  is the Bessel function and  $K_0$ ,  $I_0$  are modified Bessel functions  $K_0(-ix) = -(\pi/2)Y_0(x) + i(\pi/2)J_0(x)$ .

The Sudakov factors used in the text are defined as

$$\begin{aligned} S_{ab}(t) &= s(x_1 m_B / \sqrt{2}, b_1) + s(x_2 m_B / \sqrt{2}, b_2) + s((1 - x_2) m_B / \sqrt{2}, b_2) \\ &\quad - \frac{1}{\beta_1} \left[ \ln \frac{\ln(t/\Lambda)}{-\ln(b_1 \Lambda)} + \ln \frac{\ln(t/\Lambda)}{-\ln(b_2 \Lambda)} \right], \end{aligned} \quad (67)$$

$$\begin{aligned} S_{cd}(t) &= s(x_1 m_B / \sqrt{2}, b_1) + s(x_2 m_B / \sqrt{2}, b_2) + s((1 - x_2) m_B / \sqrt{2}, b_2) \\ &\quad + s(x_3 m_B / \sqrt{2}, b_1) + s((1 - x_3) m_B / \sqrt{2}, b_1) \\ &\quad - \frac{1}{\beta_1} \left[ 2 \ln \frac{\ln(t/\Lambda)}{-\ln(b_1 \Lambda)} + \ln \frac{\ln(t/\Lambda)}{-\ln(b_2 \Lambda)} \right], \end{aligned} \quad (68)$$

$$\begin{aligned} S_{ef}(t) &= s(x_1 m_B / \sqrt{2}, b_1) + s(x_2 m_B / \sqrt{2}, b_2) + s((1 - x_2) m_B / \sqrt{2}, b_2) \\ &\quad + s(x_3 m_B / \sqrt{2}, b_2) + s((1 - x_3) m_B / \sqrt{2}, b_2) \end{aligned}$$

$$-\frac{1}{\beta_1} \left[ \ln \frac{\ln(t/\Lambda)}{-\ln(b_1\Lambda)} + 2 \ln \frac{\ln(t/\Lambda)}{-\ln(b_2\Lambda)} \right], \quad (69)$$

$$\begin{aligned} S_{gh}(t) &= s(x_2 m_B / \sqrt{2}, b_1) + s(x_3 m_B / \sqrt{2}, b_2) + s((1-x_2)m_B / \sqrt{2}, b_1) \\ &+ s((1-x_3)m_B / \sqrt{2}, b_2) - \frac{1}{\beta_1} \left[ \ln \frac{\ln(t/\Lambda)}{-\ln(b_1\Lambda)} + \ln \frac{\ln(t/\Lambda)}{-\ln(b_2\Lambda)} \right], \end{aligned} \quad (70)$$

where the function  $s(q, b)$  are defined in the Appendix A of ref.[10].

## References

- [1] A. Gritsan, et al., CLEO Collaboration, talk at Lake Louis Winter Institute, Feb. 20-26, 2000.
- [2] H.R. Quinn and J.P. Silva, preprint hep-ph/0001290; A. Deandrea et al., preprint hep-ph/0002038; M.Z. Yang, Y.D. Yang, Phys. Rev. D62, 114019 (2000).
- [3] D.S. Du, Z.Z. Xing, Phys. Rev. D48, 4155 (1993); G. Kramer, W.F. Palmer, H. Simma, Z. Phys. C66, 429 (1995); A. Ali, G. Kramer and C.D. Lü, Phys. Rev. D58, 094009 (1998); C.D. Lü, Nucl. Phys. Proc. Suppl. 74, 227 (1999).
- [4] Y.-H. Chen, H.-Y. Cheng, B. Tseng, K.-C. Yang, Phys. Rev. D60, 094014 (1999).
- [5] C.H. Chang, H.N. Li, Phys. Rev. D55, 5577 (1997); T.W. Yeh and H.N. Li, Phys. Rev. D56, 1615 (1997).
- [6] H.N. Li, H.L. Yu, Phys. Rev. Lett. 74, 4388 (1995); Phys. Lett. B353, 301 (1995); Phys. Rev. D53, 2486 (1996).
- [7] H.N. Li, Phys. Rev. D52, 3958 (1995).
- [8] For a review, see G. Buchalla, A.J. Buras, M.E. Lautenbacher, Rev. Mod. Phys. 68, 1125 (1996).
- [9] A. Ali, G. Kramer and C.D. Lü, Phys. Rev. D59, 014005 (1999).
- [10] C.D. Lü, K. Ukai, M.Z. Yang, preprint HUPD-9924, hep-ph/0004213.
- [11] Y.Y. Keum, H.-n. Li, A.I. Sanda, preprint hep-ph/0004004; hep-ph/0004173.

- [12] Particle Data Group, Eur. Phys. J. C3, 1 (1998).
- [13] D. Cronin-Hennessy, et al., CLEO Collaboration, hep-ex/0001010; B. Aubert et al., BABAR Collaboration, hep-ex/0008057; P. Chang, Belle Collaboration, talk given at XXXth International Conference on High Energy Physics, July 27 - August 2, 2000, Osaka, Japan.
- [14] P. Ball and V.M. Braun, Phys. Rev. D58, 094016 (1998); P. Ball, J. High Energy Phys. 9809, 005 (1998).
- [15] B. Aubert et al., BABAR Collaboration, hep-ex/0008058.
- [16] M. Bander, D. Silverman, and A. Soni, Phys. Rev. Lett. 43, 242 (1979).
- [17] S. Chen, et al., CELO Collaboration, hep-ex/0001009.
- [18] M. Gronau, Phys. Lett. **B233**, 479 (1989).
- [19] R. Aleksan, I. Dunietz, B. Kayser and F. Le Diberder, Nucl. Phys. **B361**, 141 (1991).
- [20] W.F. Palmer and Y.L. Wu, Phys. Lett. **B350**, 245 (1995).